Integration of heterogeneous biological data in multiscale mechanistic model calibration: application to lung adenocarcinoma

Jean-Louis Palgen[1], Angélique Perrillat-Mercerot[1], Nicoletta Ceres[1], Emmanuel Peyronnet[1], Matthieu Coudron[1], Eliott Tixier[1], Ben M.W. Illigens[1,2], Jim Bosley[1], Adèle L'Hostis[1] and Claudio Monteiro[1*]

[1*]Novadiscovery, Pl. Giovanni da Verrazzano, Lyon, 69009, Rhône, France.
[2]Dresden International University, Freiberger Str. 37, Dresden, 01067, Germany.

*Corresponding author(s). E-mail(s): claudio.monteiro@novadiscovery.com;
Contributing authors: jean-louis.palgen@novadiscovery.com; angelique.perrillat@novadiscovery.com; nicoletta.ceres@novadiscovery.com; emmanuel.peyronnet@novadiscovery.com; matthieu.coudron@novadiscovery.com; eliott.tixier@novadiscovery.com; ben.illigens@novadiscovery.com; jim.bosley@novadiscovery.com; adele.lhostis@novadiscovery.com;

Abstract

Mechanistic models are built using knowledge as the primary information source, with well-established biological and physical laws determining the causal relationships within the model. Once the causal structure of the model is determined, parameters must be defined in order to accurately reproduce relevant data. Determining parameters and their values is particularly challenging in the case of models of pathophysiology, for which data for calibration is sparse. Multiple data sources might be required, and data may not be in a uniform or desirable format. We describe a calibration strategy to overcome the challenges of scarcity

and heterogeneity of calibration data. Our strategy focuses on parameters where initial values cannot be easily derived from the literature and where final values are estimated via calibration with constraints set by relevant data. When combined with a covariance matrix adaptation evolution strategy (CMA-ES), this step-by-step approach can be applied to a wide range of biological models. We describe a stepwise, integrative and iterative approach to multiscale mechanistic model calibration, and provide an example of calibrating a pathophysiological lung adenocarcinoma model. Using the approach described here we illustrate the successful calibration of a complex knowledge-based mechanistic model using only the limited heterogeneous datasets publicly available in the literature.

Keywords: Knowledge-based models, calibration, parameterization, lung adenocarcinoma

1 Introduction

Multiscale mechanistic modeling is an approach that bridges physiology and pathophysiology across multiple spatial scales and physical processes (Eissing, 2011; Buil-Bruna et al., 2015; Musante et al., 2016; Boissel et al., 2015) and is also called knowledge-based modeling. Knowledge-based models (KBMs) capture the complexity of biological functions in one or several subparts of a mechanistic model, using a broad range of knowledge (see Box 1) extracted from data.

Box 1: Definitions of modeling-related terms

Parameter: quantitative entity within a model whose value is set to remain constant in a particular context. For example, an IC50 value might represent the drug concentration yielding half-maximal tumor growth inhibition.
Variable: quantitative entity within a model, which value depends on parameters and/or other variables and is expected to vary with time. For instance, the number of cells in a tumor may vary in response to treatment or immune system activity.
Phenomenon: biological process defined by its given inputs, outputs, and granularity level (*e.g.* a metabolic pathway or circulation of one entity).
Data: structured observation with qualitative or quantitative information from a defined set of subjects (*e.g.* patients). It refers to the information obtained from a single statistical unit in an observational study (*e.g.* cohort, survey, -omics study) or an experiment (*e.g.* animal experiment, *in vitro* experiment, clinical trial).
Knowledge: structured information about a phenomenon that is derived from several observations and/or experiments. It can refer to an entity (*e.g.* an ionic channel, a gene), a relationship (*e.g.* an ionic current which brings a signal from entity X to entity Y) or a phenotype/genotype for instance. A piece of established knowledge, also called a scientific fact (*e.g.* the immune system consists of several cell types) is based on multiple observations and experiments (*i.e.* data) and is therefore considered at the top level of evidence.
Virtual Patient: vector of parameter values that can characterize an individual from the model perspective.

KBMs rely on mathematical equations composed of parameters to mechanistically represent biological phenomena through the changes over time of biological variables (Box 1). Many of these variables can be measured experimentally (*e.g.* evolution of glucose concentration in the plasma), while others are difficult to quantify in an experimental settings (*e.g.* concentration of intracellular ATP in a specific cell) (Brown et al., 2018). To confidently draw conclusions from modeling analysis, the measurable variables of the model must reproduce what is observed in experimental settings, and the knowledge used to link measurable and non-measurable variables must be consistent with the scientific consensus. While the latter is ensured if the model is well constructed, the former can only be achieved by defining and adjusting parameter values that enable model measurable variables to reproduce the desired behavior, that is to say what is observed in experimental settings. Two methods are commonly used to find the parameter values (Box 1): parameterization and calibration (Box 2).

Box 2: Definitions of calibration-related terms

Parametrization: selection of parameter values based on human literature curation, either directly referenced values or extrapolation using assumptions (*e.g.* taking a similar value from other analogous biological entities).
Biological constraint: biological behavior identified in experimental data or knowledge, that the model is designed to reproduce.
Computational constraint: computational translation of a biological constraint into numerical expression. Each computational constraint can be evaluated in a given virtual patient and generates an associated score (see calibration score).
Calibration: an automatic process in which parameters values that are a priori unknown are refined through numerical optimization routines run in parallel in order to achieve a desired behavior of the model.
Calibration score: when a computational constraint is evaluated, a numerical value or score between 0 (the constraint is not fulfilled) and 1 (the constraint is fully fulfilled) is generated for each virtual patient. Each score can be weighted to reflect a user-defined relative importance compared to other scores. For a given virtual patient, the objective function to be maximized is expressed as the weighted sum of all its scores.
Parameter space: number of parameters and their possible range within the model. Because parameters are based upon biology, their range should be limited to what is biologically possible. The size of a parameter space refers to both the number of parameters, their ranges and the complexity of their interactions (*e.g.* linear vs non-linear interactions).

The term parametrization can be applied to describe human curation used to search the scientific literature and to select representative parameter values. In contrast, calibration is an automatic numerical procedure, in which *a priori* unknown and estimated parameter values are concomitantly refined to reproduce the desired model's behavior, usually via an iterative process. Calibration constrains the dynamic behavior of the model (*e.g.* during simulation) by finding a set of parameter values that allows the model to represent biological behaviors consistent with the literature. While parametrization can be appropriate for models with a small number of parameters, calibration allows one to address models featuring a large parameter space (Box 2). Multiscale mechanistic KBMs are generally part of this second category of models and thus are subject to calibration (Box 3).

Box 3: Definitions of modeling approaches and model constraints

Knowledge-based models (KBMs) vs data-driven models (DDMs): The difference between KBMs and DDMs lies in how the models are founded/implemented: mathematical equations that represent knowledge on each biological interaction of interest for the former, and a statistical model that is assumed to fit with the data and the way they were collected for the latter. As such, KBMs are composed of parameters and variables that have plausible physiological meaning (with a potential exception if some phenomena are represented at a high level *i.e.* without mechanistic details).
Calibration *vs* fitting: model fitting, as used in DDMs, is often based upon unconstrained modification of both the model and the related parameters to minimize a metric of fit representing the difference between measured biological entities and their modeled equivalent. For instance, for population pharmacokinetic (PopPK) models, all subjects are fit at once to yield parameter distributions that minimize a weighted sum of squared errors or other metric. By contrast, calibration is more adapted to KBMs composed of parameters and variables that have physiological meaning. It is applied on a model structure deduced from knowledge, and consists in minimizing the difference between measured physiological data and modeled variable dynamics upon constrained parameter value modification, based on variable behavior. While fitting is normally done on a limited number of variables (*e.g.* drug concentration and clinical outcome), calibration explores an additional set of constraints (such as model variables remaining physiologically plausible) to ensure more robust predictions.

The objective of KBM calibration is to find the set of parameter values that allow the model variables to reproduce the desired biological behavior, that is to say a set of qualitative and quantitative knowledge and data extracted from the literature. However, knowledge and data found in literature are scarce, therefore the aim of this article is to establish a calibration strategy for existing non-calibrated computational models, using publicly available heterogeneous data to accurately estimate model parameters' values or distributions. During the process, the model architecture itself is assumed to remain static (in other words, no refactoring of the model, such as adding, removing or replacing a biological phenomenon is allowed to occur), and only the parameter values are changed. The general calibration strategy will be presented, followed by its application to a multiscale mechanistic model of lung adenocarcinoma (LUAD).

2 Methods

2.1 Mechanistic modeling

Mechanistic models are based on knowledge retrieved from literature, and represent, notably through model parameters values, well-described biological relationships between all model variables, the so-called biological phenomena (Box 1). The values of the model parameters therefore need to be correctly estimated for the model to reproduce the biology. The initial parameter identification provides plausibility of value ranges for parameters and should as much as possible be assessed on physiological knowledge. Initial values can be generated or inferred using known relationships or by hypotheses (*e.g.* via analogy, scaling). Parameters can then be classified in four categories based on the way their initial value is estimated (Yugi, 2013) (see Table 1).

Table 1 Definition of the different model parameter categories. Adapted from Yugi *et al.* (Yugi, 2013)

Class #	Description	Value implementation in the model
Class 0	Parameters with values directly reported in the literature	Parametrization (with the assumptions mentioned for classes 1 & 2)
Class 1	Parameters with values estimated from several values in the literature	
Class 2	Parameters with values estimated from the values of analogous entities in the literature	
Class 3	Parameters with values estimated via fitting to constraints	Calibration

For class 0, 1 and 2 parameters, the initial value can usually be set through parametrization based on data from the literature (see Table 1).

In this article, we will focus on finding through calibration the class 3 parameter values that allows the model to reproduce desired biological behaviors. Finding the data required to represent such expected biological behaviors requires a thorough review of the scientific literature. This step is nevertheless needed to obtain qualitative and quantitative knowledge and data that can be used to constrain the model behavior. A model is said to be calibrated when the computational constraints derived from the review are achieved.

The information found in literature usually follows one of these three formats: text descriptions, numerical values, or graphical values. All three can be converted into computational constraints. This step is crucial, as the predictive power of a mechanistic model depends on the quality and consistency of the computational constraints on which the model is evaluated. The exercise is also critical in ensuring that models fulfill biological constraints that are meaningful to the future application of the model.

2.2 Multiscale modeling

Multiscale models describe a complex process across multiple scales of time and space, and account for how quantities transform as we move from one scale to another (Bhattacharya and Viceconti, 2017; Horstemeyer, 2009).

The adequacy between the model variables and the relevant biological entities is a matter of ensuring that the model operates within the computational constraints. Depending on the level of knowledge available on some phenomena, distinct scales or levels of details (*e.g.* molecular or cellular) may coexist in a single model.

If a model does not include a variable that exactly matches some experimental entity of interest, a synthetic variable can be added. This could be something as simple as a unit conversion, or may require an additional assumption on the model. This makes it possible to evaluate quantitatively the consistency of model behavior with a broader array of computational constraints.

2.3 Calibration approach

The knowledge and data used to define the computational constraints are heterogeneous and can have different levels of granularity. To overcome this discrepancy, it is then relevant to approach the calibration of a model as a list of successive steps, each step having as its objective a specific model variable behavior matching one or more specific computational constraints. Since calibration steps are executed sequentially, the first calibration steps are prerequisites for the following steps. The order of the calibration steps is therefore important and the first steps should focus on reproducing the computational constraints related to:

- biological phenomena that are well-detailed in the literature
- biological phenomena represented with the lowest level of granularity
- biological phenomena that are less connected to the others, such as a subpart of the model that is less connected to the others

Most often, at each step one calibrates subparts of the model (also called submodels). Later steps combine these submodels to calibrate larger and larger models.

Each of the calibration steps reduces the remaining space of the parameters to be estimated. A calibration step starts with a number of parameters for which we have large uncertainty (a wide range of possible values). The calibration then either sets a definite value for that parameter (reducing the number of unknowns in the consecutive calibration steps) or it reduces the possible range of values for a parameter, limiting the plausible parameter space. Some computational constraints may influence multiple calibration steps, as each new step in the calibration should ensure that the results from the previous steps are still relevant; *i.e.* the constraints used at one step should still be verified in subsequent steps. Overall, the feasibility of a model calibration

depends on the amount and quality of the experimental data used to define the computational constraints. An illustration of such a calibration strategy is provided in Figure 1.

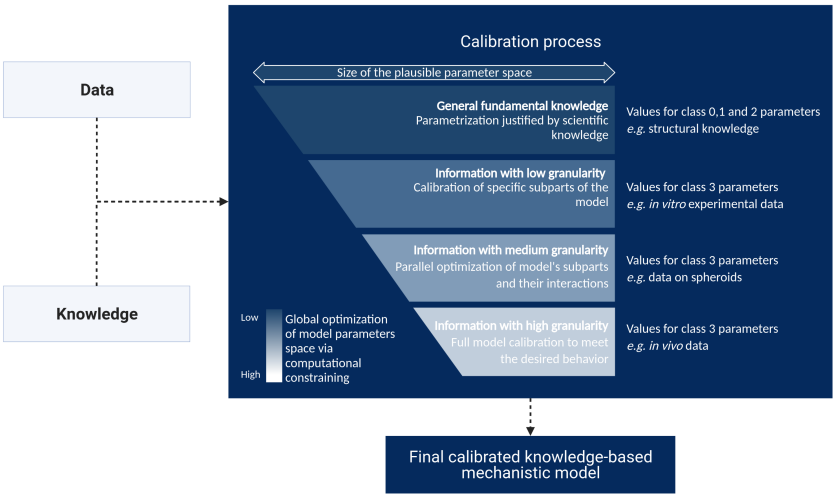

Fig. 1 Illustration of the stepwise calibration process of a model with knowledge and data as input. We propose an iterative calibration process where the size of the plausible parameter space decreases at each step, and the effect of the computational constraints applied to the model on the efficiency of the calibration process increases. Parameter classes refer to Table 1

At the end of a calibration step, the model parameter values should ensure that the model reproduces the biological behavior defined by the computational constraints.

At the end of the calibration process the model should be able to reproduce the pathophysiology of interest, in the desired context of use, represented by the whole set of computational constraints (Morrison et al., 2019).

2.4 Optimizing automatically parameters values

2.4.1 Calibration algorithm

The calibration is carried out using the Covariance Matrix Adaptation Evolution Strategy (CMA-ES) algorithm, a continuous optimizer belonging to the evolutionary methods family (Hansen et al., 2003; Jdrzejewski-Szmek et al., 2018; Tomasoni et al., 2021).

First, satisfaction of the computational constraints is translated into a maximization problem. The unknowns of the maximization problem are the values of the parameters to be calibrated. To perform the calibration, the value of parameters to be calibrated are sampled in an iterative process, and an objective value is computed based on the computational constraints. Calibration is deemed satisfied when the model outputs accurately reproduce the biological

behavior depicted by the computational constraints (Allen et al., 2016; Rieger et al., 2018).

For each model simulation, a score (Box 2) between 0 and 1 is attributed to each computational constraint: a score of 0 means the constraint is not satisfied and 1 means it is fully satisfied. Some computational constraints may have continuous scores between 0 and 1.

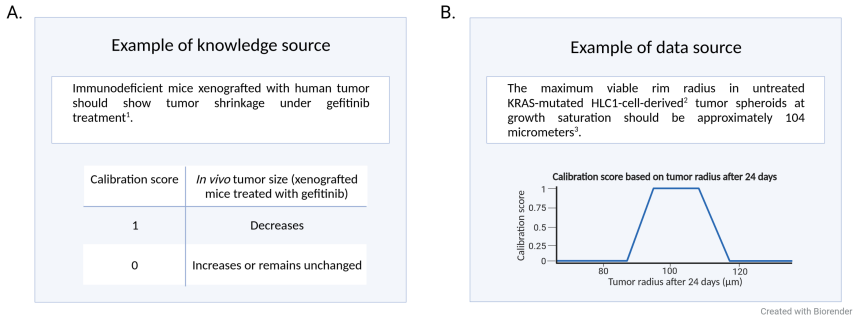

Fig. 2 Examples of transposition of biological constraints into computational constraints. A. Example of computational constraint based on knowledge, B. example of computational constraint based on experimental data. References: 1. (https://www.accessdata.fda.gov/drugsatfda_docs/label/2018/206995s003lbl.pdf); 2. (https://web.expasy.org/cellosaurus/CVCL_5529); 3. (Freyer, 1988).

Each computational constraint is weighted to reflect a user-defined importance compared to the others. For a given virtual patient, the objective function to be maximized is expressed as the weighted sum of all its scores. The objective function f is defined as:

$$f(\theta) = (1 - g(\theta))^2 \tag{1}$$

where $g(\theta)$ is referred to as the $weighted_score$ is computed as follows:

$$g(\theta) = \frac{\sum_k \omega_k \sum_b w_b s_k(y_b(\theta))}{\sum_k \sum_b \omega_k w_b} \tag{2}$$

where $y_b(\theta)$ is the model output for scenario branch b, wb its associated weight, s_k the kth sub-score and ω_k its associated weight.

Initial guesses for the parameters values are provided by the user and the CMA-ES optimizer samples new values at each iteration of the maximizing process. Maximization iterations stop when one of the following two criteria is satisfied:

- the cost function reaches a user-defined threshold
- the cost function stagnates over multiple iterations (Hansen and Kern, 2004)

2.4.2 Objective function maximization illustration

In this section we exemplify the concept of objective function maximization using the following objective function:

$$f\left(x_1, x_2\right) = -\left(4 - 2.1x_1^2 + \frac{x_1^4}{3}\right)x_2 - x_1x_2 + \left(4 - 4x_2^2\right)x_2 \tag{3}$$

This objective function features local and global maxima as shown in Figure 3 which makes it interesting to highlight the convergence properties of the CMA-ES algorithm.

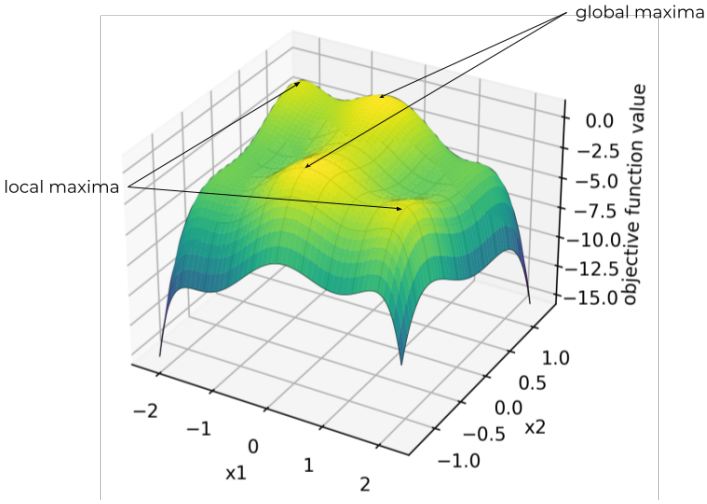

Fig. 3 Surface plot of the example objective function $f(x1, x2)$ featuring both local and global maxima (note: the same maximal value is reached twice for $(x1, x2) = (0.0898, -0.7126)$ and $(x1, x2) = (-0.0898, 0.7126)$).

In the context of calibration, the global maximum of the objective function is sought such that the model optimally matches the computational constraints. The CMA-ES algorithm, as an evolution strategy, is more suited to find such a global maximum compared to gradient-based approaches which are more likely to converge to local maxima, such as gradient descent (Galtier and Wainrib, 2013) or stochastic gradient descent (Göttlich and Totzeck, 2021).

Figure 4 shows an example of CMA-ES maximization starting from an initial guess at iteration 0 until converging to one of two global maxima at iteration 20. Despite the presence of local maxima, the CMA-ES algorithm is able to converge to a global maximum.

Figure 5 shows the evolution of the objective function values associated with the CMA-ES candidate samples throughout the iterations.

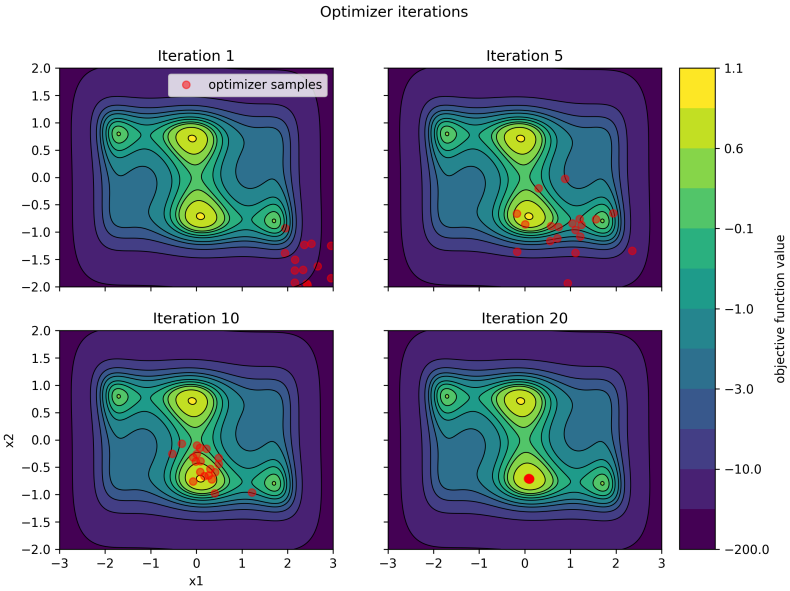

Fig. 4 Contour plots of the objective function and CMA-ES candidate samples at different iterations. The figure shows convergence to one global maximum after 20 iterations.

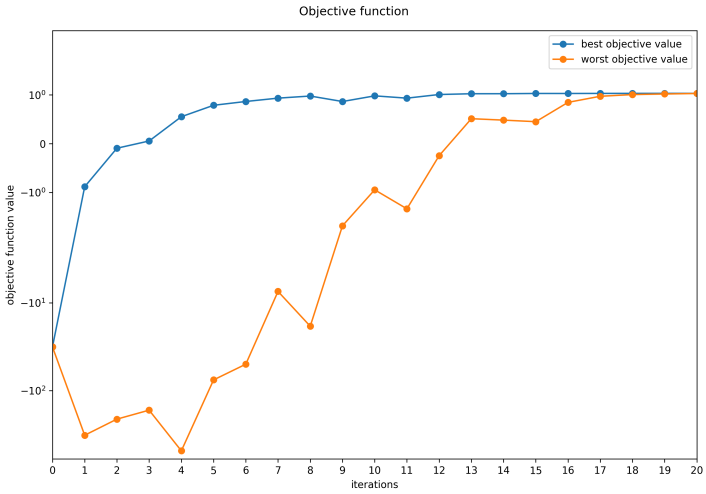

Fig. 5 Evolution of the objective function with CMA-ES iterations. For each iteration, the CMA-ES algorithm draws and evaluates the score (or objective value) of several sets of parameter values, sampled around the best set of parameter values from the previous iteration. The worst and best samples for each iteration are plotted to illustrate that a) CMA-ES finds in few iterations regions with high objective values and b) the drawn samples converge to the neighborhood of the global maximum.

3 Application example

3.1 Context: mechanistic model of lung adenocarcinoma under gefitinib treatment

Non-small-cell lung cancer (NSCLC) is the most common type of lung cancer accounting for 80-90% of all lung cancers, and about 40% of all lung cancers are adenocarcinomas (LUAD)(ESMO, 2019). These tumors start in mucus-producing cells that line the airways. The studied model, referred to as the *in silico* EGFR+ Lung Adenocarcinoma (ISELA) model, relies on a mechanistic representation of tumor evolution, from specific mutations to tumor size evolution. It additionally includes tumor shrinkage in response to administration of the first generation epidermal growth factor receptor tyrosine kinase inhibitor (EGFR-TKI) gefitinib (Lynch et al., 2004; Paez et al., 2004). We calibrated the ISELA model in order to predict tumor size evolution.

We describe here the two-step calibration that we applied to the ISELA model in order to ensure the model was reproducing the EGFR+ LUAD cell growth observed experimentally and described in literature.

3.2 Calibration protocol

3.2.1 Parametrization of class 0, 1 and 2 parameters

Within the ISELA model, the effect of mutations on the EGFR pathway was retrieved from the scientific literature and implemented as such, using parameterization. Here we present the main mutations used in the different calibration settings:

- KRAS mutation, which decreases by 97-99% (rounded to 98%) the hydrolysis of GTP once KRAS is activated (Hunter et al., 2015)
- EGFR, exon 19 deletion, which has 3 distinct effects: it leads to the constitutive activation of EGFR (Harrison et al., 2020), it alters EGFR affinity for ATP from approximately 5.0µM to 129µM (Carey et al., 2006), and it modifies the affinity of EGFR to gefitinib changing the inhibition constant from approximately 16.4 nM to an estimated 0.833 nM based on an IC 50 of 6nM (Yasuda et al., 2013), making it sensitive to gefitinib treatment (Lynch et al., 2004)
- PIK3CA mutation, leading to an estimated 2.7 fold increase of PI3K complex activity (Yamamoto et al., 2008) conferring a resistance to gefitinib (Re et al., 2019)

3.2.2 Assessing the calibration data for the ISELA model

We reviewed the scientific literature to retrieve the relevant experiments and biological phenomena related to the tumor growth in EGFR+ LUAD patients and their TTP. Five biological phenomena were identified as relevant to represent them in the context of development of the ISELA model:

1. tumor cell proliferation
2. tumor cell death
3. neoangiogenesis
4. effect of the immune system on the tumor
5. treatment

Together, these phenomena are represented with 14 parameters (see Table 2), for which we aimed to find a single value corresponding to a mean behavior within the population.

A structured review of the relevant papers, given the context of use of the ISELA model, was performed. Table 3 lists the papers that were used for the calibration of tumor growth. These tumor growth-related experimental data can be divided in two categories:

1. ***In vitro* tumor growth data** (Jagiella et al., 2016). In this experimental context, only tumor cell proliferation and death can be followed. The main assumption is that the tumor can be represented as a spherical shape and grows proportionally (Lewin et al., 2018). The two remaining biological processes related to tumor growth, namely neoangiogenesis and the effect of the immune system on the tumor, are assumed not to operate in such an *in vitro* context and are thus set to null in the simulation.
2. ***In vivo* tumor xenograft mouse model growth data** (Kang et al., 2018). In this experimental context, tumor cell proliferation and death can be followed, as well as neoangiogenesis. Immunocompromised mice were ectopically xenografted with patient-derived NSCLC tumors. We selected data for such patient-derived tumors, one carrying EGFR exon 19 deletion mutation only, thus sensitive to gefitinib, one having both the exon 19 EGFR deletion and a mutation in PIK3CA (a subunit of PI3K complex, activating the PI3K/AKT pathway), thus resistant to gefitinib. Tumor size was measured once or twice per week using a vernier caliper. The effect of the immune system on the tumor is limited (due to immunosuppression), but not null. For the data we focus on mice treated with gefitinib at 25mg/kg or injected with 5 mM citrate buffer as a placebo, by oral gavage.

The experimental data used here present the following advantages:

- They are based on cells extracted from EGFR+ LUAD human tumors.
- Tumor growth is followed either without any treatment with gefitinib which matches the context of use of the ISELA model.
- The type of EGFR+ mutation of the tumor is specified.

3.2.3 Ensuring that the model adequately represents data

Numbers of living, proliferative and dead cells are direct outputs of the ISELA model. The tumor volume is a direct output of the model:

$$tumor_{volume} = \frac{(nb_{pc} + nb_{qc} + nb_{nc})}{cancer_{cd}}$$

Table 2 Correspondence between the 14 parameters described in the table, and the five selected relevant biological phenomena.

Parameter description	Phenomena related to
Maximal depth of the tumor at which cells can survive without neoangiogenesis	tumor cell proliferation, tumor cell death
Ratio of living cells over proliferating ones with the tumor	tumor cell proliferation
Growth rate of the tumor	tumor cell proliferation
Transduction of EGFR signaling into growth signaling, first parameter: equivalent to the signal required to reach half the maximal growth	tumor cell proliferation
Transduction of EGFR signaling into growth signaling, second parameter: equivalent to the sensitivity of tumor growth to change in EGFR signal	tumor cell proliferation
Death rate of the hypoxic tumor due to necrosis	tumor cell death
Transduction of EGFR signaling into cell survival signaling, first parameter: equivalent to the signal required to reach half the maximal growth	tumor cell death
Transduction of EGFR signaling into cell survival signaling, second parameter: equivalent to the sensitivity of tumor growth to change in EGFR signal	tumor cell death
Maximal cell death inhibition the EGFR cell survival signaling can provide	tumor cell death
Number of cells neoangiogenesis can supply within the tumor	neoangiogenesis
Immune system cell killing, first parameter: maximal speed of tumor cell killing by the immune system	effect of the immune system on the tumor
Immune system cell killing, second parameter: affinity tumor cell killing by the immune system	effect of the immune system on the tumor
Immune system cell killing, third parameter: maximal number of cells the immune system can have access to	effect of the immune system on the tumor
Fraction of unbound gefitinib drug within the tumor	treatment

Table 3 References used for the calibration of tumor growth, focusing on implemented constraints on tumor size. § rim size = distance between tumor core and tumor surface

Author (year)	Study type	Biological processes
(Jagiella et al., 2016)	*in vitro* & *ex vivo*	Tumor spheroid growth curves, Fraction of proliferative cells at maximal radius
(Ekert et al., 2014)	*ex vivo*	Evolution of the proportion of proliferative cells within the tumor
(Freyer, 1988)	*in vitro*	Estimation of the viable rim size§ of the tumor
(Kang et al., 2018)	*in vitro*	Tumor volume evaluation

with nb_pc the number of proliferating cells, nb_qc the number of quiescent cells, nb_nc the number of necrotic cells, $cancer_cd$ the density of cancer cells, which is assumed to be constant within the tumor and over time as $2.8e^8$ cells/cm^3 (Grassberger et al., 2019).

Furthermore, under the assumption that the tumor shape is a perfect sphere, the tumor radius is also a direct output of the model. Consequently, under the two aforementioned assumptions, there is a direct match between the nature of the data reported in the selected papers, and the nature of the model outputs.

3.2.4 Definition of the objective of the calibration steps

As mentioned previously, the goal of the calibration for the ISELA model was to reproduce the EGFR+ LUAD cell growth described in literature and observed experimentally.

The experimental data found in literature to characterize EGFR+ LUAD tumor growth are either obtained from *in vitro* spheroids, or from xenografted mice. We therefore decided to split the ISELA calibration into two sequential steps:

- Step 1: Reproduce the tumor radius evolution and the proportion of viable cells of *in vitro* spheroids. Step 1 addresses *in vitro* scale; it focuses on tumor growth in the absence of extracellular signals related to neoangiogenesis, immune system or treatment
- Step 2: Reproduce the tumor volume evolution of human EGFR+ LUAD tumor cells transplanted into immunocompromised mice. Step 2 addresses *in vivo* scale; it focuses on tumor growth in the presence of neoangiogenesis, immune system or treatment

The scale of the model changes between step 1 and step 2 as we consider more biological phenomena. We therefore calculated part of this experimental variability using allometry theory. Allometry describes how the characteristics of living creatures such as morphological and physiological traits change with their size. Kleiber's law states that the metabolic rate scales to the $\frac{3}{4}$ power of the animal's mass for a wide range of species. Scaling laws are since then most often described with power law relationships $Z = a \times M^b$ with Z the

studied characteristic, M the organism mass, and a and b parameters called allometric coefficient and allometric exponent respectively (Pérez-García et al., 2020; Smil, 2000). Allometric scaling thus provides a way to link parameters of individuals even when they are of different species. We decided to consider allometry in our model since this framework allows us to compare species on the basis of their body weight. In this study we used a reference body weight of 2.63g for *in vitro* experiments (West, 2002) and 23g for a mouse weight (Vellers et al., 2017).

3.2.5 Automation of parameter value optimisation

Optimization of parameter values was performed automatically using the CMA-ES algorithm as described in the methods section.

3.3 Results

3.3.1 Step 1: Reproduction of tumor growth (*in vitro* spheroid data)

The evolution of tumor radius prior and after calibration was compared to the experimental data used for calibration (see Figure 6). The experimental data showed an increase of tumor radius of approximately 12.5µm/day over the first 20 days, to reach 400µm, which then started to plateau. Pre-calibration of the model showed an increase of approximately 8µm/day. After calibration, as described in the calibration protocol section, the model showed an increase of approximately 12.5µm/day and the tumor radius stayed approximately within two standard deviations of the experimental data.

Overall, the calibration showed good agreement with experimental data post calibration, reproducing the expected growth of *in vitro* KRAS-mutated spheroids, at least for the first 30 days of the experiment.

3.3.2 Step 2: Reproduction of tumor growth (*in vivo* xenograft growth data)

Evolution of tumor volume prior and after calibration was compared to the experimental data used for calibration for each of the four scenarios: EGFR mutation with or without gefitinib, EGFR and PIK3CA mutation with or without gefitinib (see Figure 7). In EGFR tumors, treated with placebo, the experimental data showed an increase of tumor volume of approximately 20mm^3/day over the first 20 days (Figure 7, A). Under gefitinib in tumors with EGFR mutation only, volume decreased in size of roughly 16mm^3/day over the first 10 days, before plateauing (Figure 7, B). In tumors with both EGFR and PIK3CA mutations, treatment with gefitinib showed no effect compared to placebo with tumor volume increasing roughly by 7.5mm^3/day over the first 20 days (Figure 7, C and D).

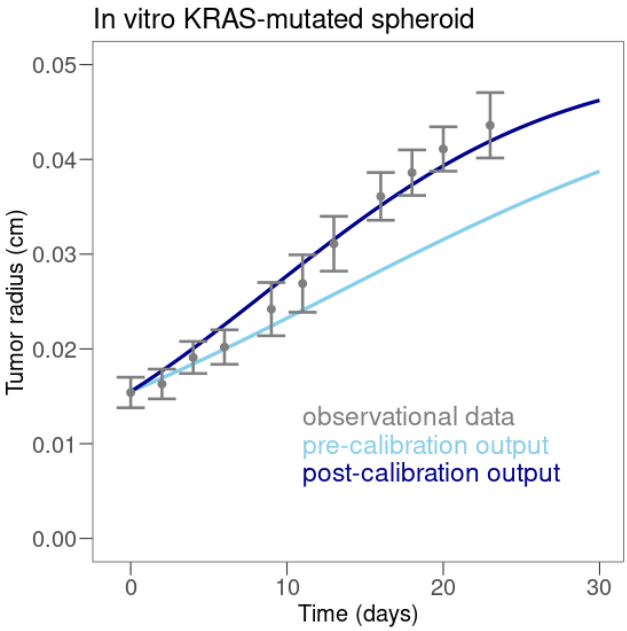

Fig. 6 Efficacy of calibration of tumor radius on *in vitro* spheroids carrying KRAS mutation. Experimental data are shown in gray (error bars represent 2 standard deviations, experimental data are reported by Jagiella et al. (2016), simulated data prior to calibration in light blue and simulated data after calibration in dark blue.

Overall, this calibration step successfully reproduced the growth of two xenografted tumors carrying EGFR exon 19 deletion, and one having in addition a mutation in PIK3CA, as reported in Kang et al. (2018). The simulation could reproduce not only tumor evolution with placebo but also the differential effect of gefitinib depending on the tumor genotype.

The calibration thus succeeded in allowing the model to faithfully reproduce observed experimental data and fulfill the associated computational constraints. The changes in parameter values are detailed in the supplementary material.

4 Discussion

In mechanistic modeling, calibration as we present it here is not part of the standard protocol, although it could help to improve predictions and model reusability by improving its adequacy to the knowledge and data from literature. A perspective about QSP models emphasizes the need to formalize model development and verification aspects and highlights optimal structural granularity and parameter estimation as critical aspects (Ribba et al., 2017). Calibration methodology, however, is often insufficiently discussed. If calibration is described, no standardized or generalized method is employed.

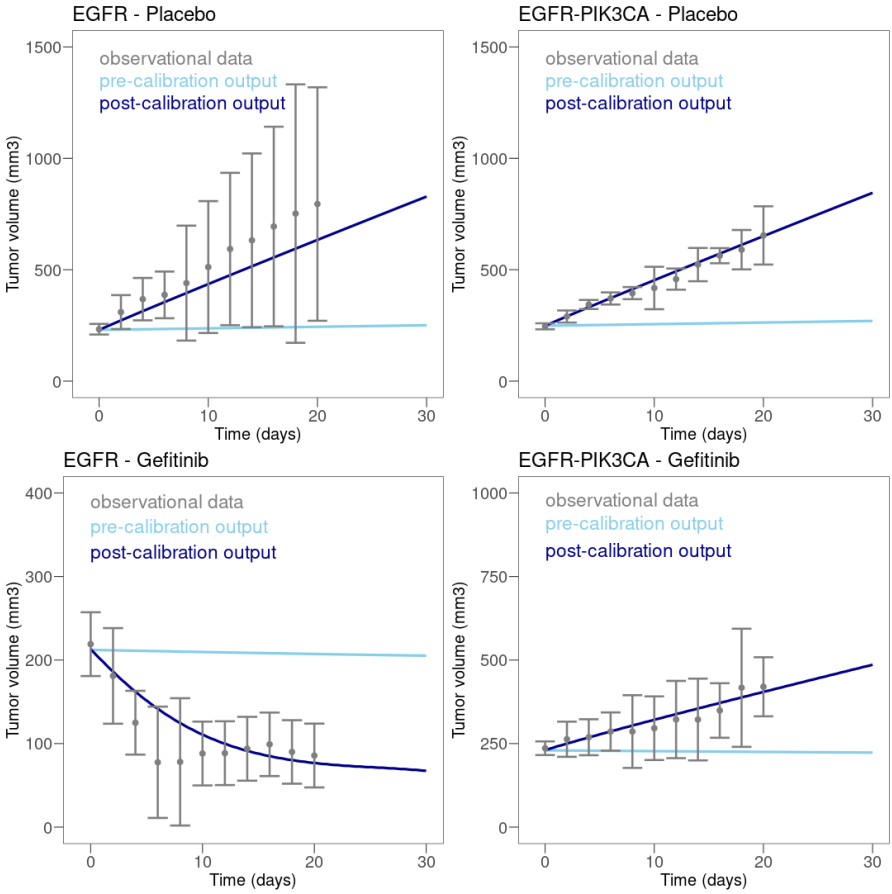

Fig. 7 Efficacy of calibration of tumor volume with xenograft data. On each plot, the experimental data are shown in gray (Error bars on experimental data correspond to 2 standard deviations of the data reported in Kang et al. (2018)), simulated data prior to calibration in light blue and simulated data after calibration in dark blue. The type of mutations carried by the tumor is indicated on top of each plot.

Frequently, identifying the appropriate data set for calibration is a major challenge. Only a few papers could be identified with a detailed description of the calibration process. In a mathematical model of blood eosinophil dynamics calibration was performed against *in vitro* and *in vivo* data (Karelina et al., 2016). Willis *et al.* have used parameter regression methods to calibrate an SIRD model for COVID-19 (Willis et al., 2021). For a mechanistic model of oral poliovirus-related vaccine virus transmission risk, optimal model parameters were identified with Latin hypercube sampling and a pseudo-likelihood function to minimize the discrepancy between simulated and observed data (Famulare et al., 2021).

In this paper, we present a calibration methodology where the benefits of heterogeneous types of data are leveraged through (1) data assessment,

(2) assurance of satisfying adequacy between model and observed data, (3) definition of the aim of each calibration step, (4) automatic optimization of parameters, and (5) integration of all calibration steps. The resulting calibration protocol addresses (1) data with different degrees of precision, from individual measurements to general knowledge, (2) data with different provenance (*in vitro* or *in vivo* and from several species), (3) data with different granularity (individual record or population-based), and (4) calibration at different levels, *i.e.* calibration of all measurable variables, regardless of their granularity.

From a theoretical perspective, the main limitations of such an approach are the availability of relevant knowledge and consistent data to efficiently constrain the model. In particular, when the biological constraints from literature are in disagreement, it may indicate that the respective phenomena are not sufficiently characterized in the literature. A documented removal of constraints or changes in the model structure may be viable options. Also, some phenomena may not be sufficiently documented in the literature, leading to a lack of computational constraints. In such a case, drawing some documented simplifying assumptions, or exploring alternative explanatory hypotheses, may be critical in model development and calibration.

The calibration strategy proposed in this paper can be compared to the use of machine learning (ML) in model development. ML model development is more standardized and includes training, testing and validation of a model. A training dataset is used initially to fit the model parameters. The model is then optimized on a training dataset with methods such as gradient descent to adjust model parameters. The fitted model is finally validated with a validation dataset where the model's predictions are compared with the responses for the observations. In ML, similar to mechanistic modeling, lack of data is often the main limitation (Roh et al., 2021). Especially in healthcare, data-driven ML is limited due to bias and data access due to privacy concerns, data silos and heterogeneous data formats (Rieke et al., 2020).

From a technical perspective, there are two additional aspects that need to be considered for mechanistic modeling: the computational cost and the global convergence verification of the process. Calibration of many parameters requires significant computational power and a significant amount of available data. Therefore, a parsimonious approach to model building with reducing the number of class 3 parameters to calibrate (*e.g.* through simplifying assumptions, or sensitivity analysis to identify parameters affecting the outcome(s) of interest the most) is a key step. Also, a thorough exploration of calibration algorithm settings is necessary to ensure that the calibration converges to a unique set of values and that this convergence corresponds to a global maximum of the cost-function. Otherwise, if left unverified, the process may not have converged at all, or will have converged to a local maximum, leading to a suboptimal performance.

The stepwise process as presented here allows the calibration of increasingly larger models, starting from a relatively basic one to a more complex one.

Those calibration protocols lead to the production of independent reusable subparts of models as well as complex models as a whole. These models can be reused in other contexts as a starting point to build calibrated mechanistic models adaptable to the available data and questions of interest. The method naturally produces calibrated portions of larger models, and these submodels can be used in other contexts.

We have applied this calibration strategy to a mechanistic multiscale KBM of lung adenocarcinoma harboring specific EGFR mutations, and focused on the calibration of tumor growth parameters based on *in vitro* experiments and xenografted mice. This led to the successful calibration of the model with these experimental settings as the calibrated model showed an adequate fit with the experimental data (see Figure 6 and 7). The model is currently under further development, in order to be able to represent measurements observed in humans. The ISELA model will likely require additional calibration steps focusing on specific parameters, *e.g.* to represent the human immune system. This would also imply calibrating not just the average behavior amongst the population, but also the inter-patient variability, to generate a Virtual Population matching the characteristics of a real population. To formally assess the performance of the model and its results' generalizability, validation of the model will be performed with data that were neither used for building the model nor calibration, *e.g.* real world data or clinical trial data.

After the calibration process and an additional validation procedure on an independent dataset, an additional application of a mechanistic model would be the generation of independent virtual populations to answer clinical questions *in silico*.

Acknowledgement

We would like to thank Janssen-Cilag France for supporting the project used as an example application in this article. In addition, the comments of two anonymous reviewers helped us to improve the manuscript.

References

Allen R, Rieger T, Musante C (2016) Efficient generation and selection of virtual populations in quantitative systems pharmacology models. CPT: Pharmacometrics & Systems Pharmacology 5(3):140–146. https://doi.org/10.1002/psp4.12063

Bhattacharya P, Viceconti M (2017) Multiscale modeling methods in biomechanics. Wiley Interdisciplinary Reviews: Systems Biology and Medicine 9(3):e1375. https://doi.org/10.1002/wsbm.1375

Boissel JP, Auffray C, Noble D, et al. (2015) Bridging systems medicine and patient needs. CPT: Pharmacometrics & Systems Pharmacology 4(3):135–145. https://doi.org/10.1002/psp4.26

Brown LV, Gaffney EA, Wagg J, et al. (2018) Applications of mechanistic modelling to clinical and experimental immunology: an emerging technology to accelerate immunotherapeutic discovery and development. Clinical and Experimental Immunology 193(3):284–292. https://doi.org/10.1111/cei.13182

Buil-Bruna N, López-Picazo JM, Martín-Algarra S, et al. (2015) Bringing model-based prediction to oncology clinical practice: A review of pharmacometrics principles and applications. The Oncologist 21(2):220–232. https://doi.org/10.1634/theoncologist.2015-0322

Carey KD, Garton AJ, Romero MS, et al. (2006) Kinetic analysis of epidermal growth factor receptor somatic mutant proteins shows increased sensitivity to the epidermal growth factor receptor tyrosine kinase inhibitor, erlotinib. Cancer Research 66(16):8163–8171. https://doi.org/10.1158/0008-5472.can-06-0453

Eissing T (2011) A computational systems biology software platform for multiscale modeling and simulation: Integrating whole-body physiology, disease biology, and molecular reaction networks. Frontiers in Physiology 2. https://doi.org/10.3389/fphys.2011.00004

Ekert JE, Johnson K, Strake B, et al. (2014) Three-dimensional lung tumor microenvironment modulates therapeutic compound responsiveness in vitro – implication for drug development. PLoS ONE 9(3):e92,248. https://doi.org/10.1371/journal.pone.0092248

ESMO (2019) Non-small-cell lung cancer (NSCLC). ESMO Patient Guide Series -ESMO Clinical Practice Guidelines URL https://www.esmo.org/for-patients/patient-guides/non-small-cell-lung-cancer

Famulare M, Wong W, Haque R, et al. (2021) Multiscale model for forecasting sabin 2 vaccine virus household and community transmission. PLOS Computational Biology 17(12):e1009,690. https://doi.org/10.1371/journal.pcbi.1009690

Freyer JP (1988) Role of necrosis in regulating the growth saturation of multicellular spheroids. Cancer Res 48(9):2432–2439

Galtier MN, Wainrib G (2013) A biological gradient descent for prediction through a combination of STDP and homeostatic plasticity. Neural Computation 25(11):2815–2832. https://doi.org/10.1162/neco_a_00512

Göttlich S, Totzeck C (2021) Parameter calibration with stochastic gradient descent for interacting particle systems driven by neural networks. Mathematics of Control, Signals, and Systems pp 1–30. https://doi.org/10.1007/s00498-021-00309-8

Grassberger C, McClatchy D, Geng C, et al. (2019) Patient-specific tumor growth trajectories determine persistent and resistant cancer cell populations during treatment with targeted therapies. Cancer research 79(14):3776–3788. https://doi.org/10.1158/0008-5472.CAN-18-3652

Hansen N, Kern S (2004) Evaluating the cma evolution strategy on multimodal test functions. In: Yao X, Burke EK, Lozano JA, et al. (eds) Parallel Problem Solving from Nature - PPSN VIII. Springer Berlin Heidelberg, Berlin, Heidelberg, pp 282–291, https://doi.org/10.1007/978-3-540-30217-9_29

Hansen N, Müller SD, Koumoutsakos P (2003) Reducing the time complexity of the derandomized evolution strategy with covariance matrix adaptation (CMA-ES). Evolutionary Computation 11(1):1–18. https://doi.org/10.1162/106365603321828970

Harrison PT, Vyse S, Huang PH (2020) Rare epidermal growth factor receptor (EGFR) mutations in non-small cell lung cancer. Seminars in Cancer Biology 61:167–179. https://doi.org/10.1016/j.semcancer.2019.09.015

Horstemeyer MF (2009) Multiscale modeling: A review pp 87–135. https://doi.org/10.1007/978-90-481-2687-3_4

Hunter JC, Manandhar A, Carrasco MA, et al. (2015) Biochemical and structural analysis of common cancer-associated KRAS mutations. Molecular Cancer Research 13(9):1325–1335. https://doi.org/10.1158/1541-7786.mcr-15-0203

Jagiella N, Müller B, Müller M, et al. (2016) Inferring growth control mechanisms in growing multi-cellular spheroids of NSCLC cells from spatial-temporal image data. PLOS Computational Biology 12(2):e1004,412. https://doi.org/10.1371/journal.pcbi.1004412

Jdrzejewski-Szmek Z, Abrahao KP, Jdrzejewska-Szmek J, et al. (2018) Parameter optimization using covariance matrix adaptation—evolutionary strategy (CMA-ES), an approach to investigate differences in channel properties between neuron subtypes. Frontiers in Neuroinformatics 12. https://doi.org/10.3389/fninf.2018.00047

Kang HN, Choi JW, Shim HS, et al. (2018) Establishment of a platform of non-small-cell lung cancer patient-derived xenografts with clinical and genomic annotation. Lung Cancer 124:168–178. https://doi.org/10.1016/j.lungcan.2018.08.008

Karelina T, Voronova V, Demin O, et al. (2016) A mathematical modeling approach to understanding the effect of anti-interleukin therapy on eosinophils. CPT: Pharmacometrics & Systems Pharmacology 5(11):608–616. https://doi.org/10.1002/psp4.12129

Lewin TD, Maini PK, Moros EG, et al. (2018) The evolution of tumour composition during fractionated radiotherapy: Implications for outcome. Bulletin of Mathematical Biology 80(5):1207–1235. https://doi.org/10.1007/s11538-018-0391-9

Lynch TJ, Bell DW, Sordella R, et al. (2004) Activating mutations in the epidermal growth factor receptor underlying responsiveness of non-small-cell lung cancer to gefitinib. N Engl J Med 350(21):2129–2139. https://doi.org/10.1056/NEJMoa040938

Morrison TM, Hariharan P, Funkhouser CM, et al. (2019) Assessing computational model credibility using a risk-based framework: Application to hemolysis in centrifugal blood pumps. ASAIO Journal 65(4):349–360. https://doi.org/10.1097/mat.0000000000000996

Musante C, Ramanujan S, Schmidt B, et al. (2016) Quantitative systems pharmacology: A case for disease models. Clinical Pharmacology & Therapeutics 101(1):24–27. https://doi.org/10.1002/cpt.528

Paez JG, Jänne PA, Lee JC, et al. (2004) EGFR mutations in lung cancer: Correlation with clinical response to gefitinib therapy. Science 304(5676):1497–1500. https://doi.org/10.1126/science.1099314

Pérez-García VM, Calvo GF, Bosque JJ, et al. (2020) Universal scaling laws rule explosive growth in human cancers. Nature physics 16(12):1232–1237. https://doi.org/10.1038/s41567-020-0978-6

Re MD, Crucitta S, Gianfilippo G, et al. (2019) Understanding the mechanisms of resistance in EGFR-positive NSCLC: From tissue to liquid biopsy to guide treatment strategy. International Journal of Molecular Sciences 20(16):3951. https://doi.org/10.3390/ijms20163951

Ribba B, Grimm H, Agoram B, et al. (2017) Methodologies for quantitative systems pharmacology (QSP) models: Design and estimation. CPT: Pharmacometrics & Systems Pharmacology 6(8):496–498. https://doi.org/10.1002/psp4.12206

Rieger TR, Allen RJ, Bystricky L, et al. (2018) Improving the generation and selection of virtual populations in quantitative systems pharmacology models. Progress in Biophysics and Molecular Biology 139:15–22. https://doi.org/10.1016/j.pbiomolbio.2018.06.002

Rieke N, Hancox J, Li W, et al. (2020) The future of digital health with federated learning. npj Digital Medicine 3(1). https://doi.org/10.1038/s41746-020-00323-1

Roh Y, Heo G, Whang SE (2021) A survey on data collection for machine learning: A big data - AI integration perspective. IEEE Transactions on Knowledge and Data Engineering 33(4):1328–1347. https://doi.org/10.1109/tkde.2019.2946162

Smil V (2000) Laying down the law. Nature 403(6770):597–597. https://doi.org/10.1038/35001159

Tomasoni D, Paris A, Giampiccolo S, et al. (2021) QSPcc reduces bottlenecks in computational model simulations. Communications Biology 4(1). https://doi.org/10.1038/s42003-021-02553-9

Vellers HL, Letsinger AC, Walker NR, et al. (2017) High fat high sugar diet reduces voluntary wheel running in mice independent of sex hormone involvement. Frontiers in physiology 8:628. https://doi.org/10.3389/fphys.2017.00628

West G (2002) Woodruff wh, brown jh. Allometric scaling of metabolic rate from molecules and mitochondria to cells and mammals Proc Natl Acad Sci USA 99:2473–2478. https://doi.org/10.1073/pnas.012579799

Willis MJ, Wright A, Bramfitt V, et al. (2021) COVID-19: Mechanistic model calibration subject to active and varying non-pharmaceutical interventions. Chemical Engineering Science 231:116,330. https://doi.org/10.1016/j.ces.2020.116330

Yamamoto H, Shigematsu H, Nomura M, et al. (2008) PIK3ca mutations and copy number gains in human lung cancers. Cancer Research 68(17):6913–6921. https://doi.org/10.1158/0008-5472.CAN-07-5084

Yasuda H, Park E, Yun CH, et al. (2013) Structural, biochemical, and clinical characterization of epidermal growth factor receptor (EGFR) exon 20 insertion mutations in lung cancer. Science Translational Medicine 5(216). https://doi.org/10.1126/scitranslmed.3007205

Yugi K (2013) Dynamic kinetic modeling of mitochondrial energy metabolism pp 105–142. https://doi.org/10.1007/978-1-4614-6157-9_8